Structural and electronic properties of InSb under pressure

G. Y. Guo
Daresbury Laboratory, Science and Engineering Research Council, Warrington WA4 4AD, United Kingdom

J. Crain
Department of Physics, University of Edinburgh, Edinburgh EH9 3JZ, Scotland, United Kingdom

P. Blaha
Institut fuer Technische Elektrochemie, Technische Universitat Wien, A-1060 Wien, Austria

W. M. Temmerman
Daresbury Laboratory, Science and Engineering Research Council, Warrington WA4 4AD, United Kingdom
(Received 30 June 1992)

We have investigated the structural and electronic properties of the III-V semiconductor InSb under pressure by means of first-principles density-functional total-energy calculation using the all-electron full potential linear augmented plane-wave method. We find that in the high-pressure region, the β-Sn structure is unstable and a body-centered orthorhombic structure (space group $Imm2$) is energetically more favorable. Calculated structural parameters (a/b and a/c ratios, and atomic positions) are in good agreement with a recent highly accurate x-ray-diffraction experiment using an image plate area detector. Theoretical lattice constant and bulk modulus for the normal-pressure zincblende structure is also in very good agreement with experiments. We present calculated structural properties as well as band structures and charge densities for the various structures studied. We discuss the processes of the phase transformation, and also the bonding and structural stabilities in terms of the calculated electronic properties.

I. INTRODUCTION

The III-V zincblende compounds are interesting materials with important applications in electronic devices. Like group-IV semiconductors such as Si and Ge, these compounds are semiconductors at the ambient pressure but become metallic under pressure. It is known that Si and Ge undergo a zincblende–β-Sn structural transformation under pressure.[1] A similar phase transition might be expected for the III-V zincblende compounds. Therefore, when a high-pressure structure in InSb was first observed, it was assumed to be the tetragonal β-Sn structure (or the polar analogue of the β-Sn structure).[2] This appeared to be confirmed by subsequent x-ray experiments.[3] Furthermore, a similar behavior of the valence electron densities near the transition pressure for Si and InSb was observed in x-ray-diffraction measurements.[4] Nevertheless, recent experiments with refined techniques have shown this simple picture to be incorrect.[5,6] In fact these materials exhibit rich crystal phases and behaviors under pressure. For example, it has been found that although GaP transforms to the β-Sn structure,[5] GaAs transforms from the zincblende to an orthorhombic phase[5,6] and AlP to an incompletely-determined face-centered-cubic structure.[7]

Clearly, a thorough understanding of the high-pressure properties of the III-V zincblende compounds is needed. While further accurate experimental work is necessary, first-principles theoretical work is also essential in order to gain insight at the microscopic level. In parallel with the ongoing experimental program using the synchrotron radiation source at Daresbury Laboratory,[8] a theoretical study based on first-principles density-functional theory is currently being carried out. The highly accurate full potential linear augmented plane-wave (FLAPW) method is used.[9] It has already been shown that the full potential density-functional calculations are able to predict accurate structural properties for solids ranging from semiconductors to metals.[10] Therefore, first-principles calculations should also help to resolve many plausible high-pressure structures suggested but not completely determined by previous experiments.

In this work, we focus on InSb. Because of its low-transition pressure (around 10–20 kbar) InSb is perhaps the most intensively studied compound.[3,7,11,12] Nevertheless, the high-pressure structures of InSb are still controversial. For example, early x-ray-diffraction works indicated that under pressure InSb first undergoes a transition from the zincblende to the β-Sn structure.[3] More recent experiments suggested that InSb transforms to simple orthorhombic structures.[11] An *ab initio* study of InSb using the pseudopotential method has also been carried out.[13] Several plausible high-pressure structures including simple orthorhombic structures, cubic rocksalt, hexagonal types, and also β-Sn structure, were investigated, and the β-Sn structure was found to be the stable high-pressure structure. Interestingly, a recent highly accurate powder x-ray-diffraction experiment using powerful synchrotron radiation and a x-ray area detector (called an image plate) revealed that the simple orthorhombic struc-

ture proposed earlier[11] is in fact a body-centered orthorhombic structure.[8] In the present work, we perform all-electron total-energy FLAPW calculation for an orthorhombic structure (space group $Imm2$) and the β-Sn structure as well as the cubic zincblende structure. We find that the β-Sn structure is unstable with respect to the $Imm2$ structure at high pressures.

The organization of the rest of the paper is as follows. In Sec. II, we describe the details of our calculations. In Sec. III, we report the calculated structural properties of InSb and discuss the available experimental results. In Sec. IV, we present the calculated electronic properties and compare the results for the different structures in an attempt to understand the structural properties of InSb in terms of the underlying electronic structures. Finally, a summary and conclusion are given in Sec. V.

II. COMPUTATIONAL DETAILS

We performed first-principles electronic structure and total-energy calculations for InSb within the density-functional theory[14] with the local-density approximation (LDA). The Vosko-Wilk-Nusair form[15] of the LDA exchange-correlation potential was used throughout. This is believed to be the most accurate parameterized LDA exchange-correlation potential. The Kohn-Sham equations were solved with the full potential linear augmented plane-wave (FLAPW) technique.[9] Like the *ab initio* pseudopotential method,[10,13] the FLAPW method is a widely used electronic structure method and gives accurate physical properties for a variety of solids.[16,17] In contrast to the pseudopotential, however, the FLAPW method is an all-electron technique and can also deal with systems containing rather localized valence electrons, such as transition metals and their compounds.[17] We refer to Ref. 9 and references therein for the details of the FLAPW method.

In the present self-consistent calculations, the electrons are separated into two groups, namely the "core" electrons whose charge densities are confined within the "muffin-tin" spheres and the "valence" (or band) electrons. The core electron states are treated fully relativistically by solving the Dirac equation for the spherical component of the potential. The valence electrons are treated scalar relativistically[18] (i.e., all the important relativistic effects (the mass-velocity correction and Darwin terms) except the spin-orbit coupling, are included). In contrast to previous pseudopotential calculations for III-V semiconductors,[13] the "shallow" core (or semicore) states (i.e., In and Sb $4d$ states) were also considered as bands through use of a second energy window. There is a significant proportion of the In (Sb) $4d$ charge outside the muffin-tin spheres at all volumes considered. For example, the charge density spilling out for the In $4d$ is as large as 0.4 electron. Furthermore, the energy levels of the In $4d$ states are only about 5–6 eV below the bottom of the valence bands. Thus, it is not *a priori* justified to treat the In (Sb) $4d$ electrons as core states.

The special k-point Brillouin-zone integration technique is used to evaluate new charge densities from the calculated LAPW wave functions. The special k-point sets for all the structures investigated are generated using the Monhorst-Pack scheme.[19] For the semicore bands, four, four, and six special k points are used for the cubic zincblende, β-Sn, and $Imm2$ structures, respectively. Because these bands are fully occupied, the number of k points needed is small. We find that the total energy converges to within 0.5 mRy with these sets of the special k points. For the valence bands, ten special k points are used for the cubic zincblende structure. Because this structure is semiconducting (but see Sec. IV) and the valence bands are full, this ten k-point set is again found to be sufficient. The two high-pressure structures considered are metallic. Consequently, far more special k points are required for the valence bands. We used 160 and 288 special k points for the β-Sn and $Imm2$ structures, respectively. Further increasing the number of special k points changes the calculated total energy by less than 0.5 mRy. The muffin-tin sphere radii used in all our calculations are 2.4 Bohr radius (a.u.) for In and 2.45 a.u. for Sb. Note that, since the FLAPW method is a full potential method, the final results are not dependent on the muffin-tin radii chosen. Inside the muffin-tin spheres, the wave functions, charge densities, and potential are expanded in terms of the spherical harmonics. The cutoff angular momentum ($L_{\max}$) is 12 for the wave functions, and 6 for charge densities (potentials). The number of the plane waves is determined by the $K_{\max}$ (largest wave vector). $K_{\max}=2.86$ a.u.$^{-1}$ is used for the valence bands. This gives rise to about 180 and 130 plane waves (PW's), respectively, for the cubic and noncubic structures with the minimum energy lattice constants. For the semicore bands, it turned out that far more plane waves were needed. We used $K_{\max}=4.29$ a.u.$^{-1}$. This is equivalent to have about 650 and 450 PW's, respectively, for the cubic and noncubic structures with the minimum energy lattice constants. We found that the minimum energy difference between the β-Sn and $Imm2$ structures is small (see Sec. III). To further ensure that the calculated structural energy differences are accurate, we performed a FLAPW calculation treating the β-Sn structure as the $Imm2$ structure and another one regarding the zincblende as the β-Sn structure. In both cases, the inconsistency in the total energy is less than 0.2 mRy. In summary, with this choice of the computational parameters, the calculated total energies to be presented below, converge to within 1.0 mRy with respect to both the cutoff wave vector ($K_{\max}$) and the cutoff angular momentum ($L_{\max}$), and the calculated structural energy differences converge to within 0.5 mRy.

III. STRUCTURAL PROPERTIES

Principal results of our total-energy calculations are summarized in Fig. 1 where the total energy for each structure considered is shown as a function of unit-cell volume. Small circles and squares in Fig. 1 indicate the calculated values. The three curves are the Murnaghan's equation of state[20] fitted to the calculated total energies for each structure. The bulk modulii, equilibrium lattice

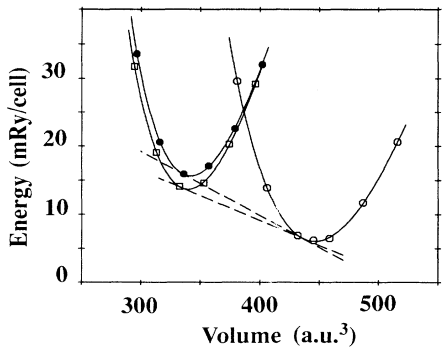

FIG. 1. Calculated total energies (relative to $E_0 = -24\,712.74$ Ry) as a function of unit cell volume for InSb in the zincblende (open circles), β-Sn (solid circles), and $Imm2$ (open squares) structures. The curves are the fitted Murnaghan's equations of state and slopes of the dashed lines give transition pressures for zincblende to β-Sn (14 kbar) and zincblende to $Imm2$ (11 kbar) (see text).

constants, and other structural properties can then be obtained from these fitted equations of state. As expected, the ground-state structure is the cubic zincblende. The calculated equilibrium lattice constant (a) is 6.42 Å, in excellent agreement with experiments (6.49 Å) (Ref. 21) (being about 1% too small). The calculated bulk modulus (B_0) is 0.52 Mbar, which is 8% too large as compared with the experimental value of 0.48 Mbar.[22] These values are also in good agreement with the previous pseudopotential calculations (a is 6.36 Å and B_0 0.47 Mbar).[13]

The β-Sn structure has the body-centered tetragonal symmetry (space group $I4m2$) (see Fig. 2). The atomic positions in the unit cell are In(0,0,0) and Sb(0,$\frac{1}{2}$,u) ($u = \frac{1}{4}$). If one increases the c/a ratio to $\sqrt{2}$, one gets the zincblende structure. Firstly, several total-energy calculations were performed for different c/a ratios. The minimum energy c/a ratio is about 0.561, being 4% larger than the experimental value of 0.539.[11] This theoretical c/a ratio was then used in calculating the β-Sn total-energy-volume curve shown in Fig. 1. In the $Imm2$ structure, there are also two atoms in the primitive cell with In(0,0,0) and Sb(0,$\frac{1}{2}$,u) (see Fig. 2). If $u = \frac{1}{4}$ and $a = b$, the $Imm2$ structure becomes the β-Sn structure. We started our calculations with the preliminary experimental structure parameters ($a = 5.816$ Å, $b = 5.362$ Å, $c = 3.161$ Å, and $u = 0.47$) measured at about 35 kbar.[8] Firstly, the minimum energy volume is determined. Secondly, we calculated the total energy as a function of u with the volume fixed to the minimum energy value. We found that the minimum energy value of u is 0.48, being almost equal to 0.47. We also found that the energy curve is very flat around $u = 0.48$ with no energy change (less than 2 meV/unit cell) for u ranging from 0.45 to 0.51. Thirdly, using a fixed volume and a fixed u of 0.47, we calculated the total energy as a function of either the a/b ratio (with a fixed c) or the a/c ratio (with a fixed a/b ratio). The final structure parameters we obtained are $a/b = 1.095$, $c/a = 0.546$. These calculated parameters are very close to the above experimental values. With these lattice parameters (a/b and c/a ratios) fixed, we finally recalculated the total energy as a function of the unit-cell volume and the results are shown in Fig. 1. Of course, the best way to obtain the theoretical structural parameters is to adjust v(volume), u, a/b, and c/a *simultaneously,* which we cannot do at present. Alternatively, one can also obtain the accurate structural parameters (u, a/b, and c/a) if one repeats the process described above until self-consistency is achieved. Since the final minimum energy volume (Fig. 1) is nearly equal to the one obtained at the beginning of the process, we believe that the structural parameters ($u \sim 0.48$, $a/b \sim 1.095$, and $c/a \sim 0.546$) given above are good estimates.

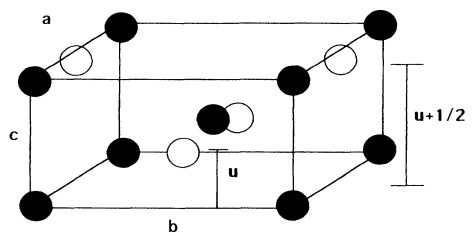

FIG. 2. The high-pressure structure of InSb. The unit cell used in the calculations is orthorhombic with space group $Imm2$ and a basis of In(0,0,0) and Sb(0,$\frac{1}{2}$,u). When $a = b$, $c/a \sim \frac{1}{2}$, and $u = \frac{1}{4}$, this structure becomes the tetragonal β-Sn structure.

Figure 1 indicates that in the high-pressure region, the $Imm2$ structure is stable whereas the β-Sn structure is not. The minimum energy difference is small (about 2 mRy/unit cell or 27 meV/unit cell), but certainly larger than our numerical uncertainties (see Sec. II). The minimum energy difference between the $Imm2$ and zincblende is about 8 mRy/unit cell. As mentioned before, several plausible high-pressure structures have been studied by Zhang and Cohen using the *ab initio* pseudopotential method.[13] These include almost all the possible structures proposed by the previous experiments.[3,11,12] Unsurprisingly, the β-Sn structure was found to have the lowest minimum energy in the high-pressure region. Thus, InSb was predicted to transform from the zincblende to the β-Sn structure. However, our present results show that the $Imm2$ structure will be the stable high-pressure structure of InSb.

Interestingly, we find that the β-Sn structure is stable against two following orthorhombic distortions. We performed several total-energy calculations first for a set of different (a,b) values with a fixed u of $\frac{1}{4}$ and then for a set of different u values with $a = b$. In these calculations, the volume is fixed to the minimum energy volume (Fig. 1). The results show that the β-Sn structure always has the lowest total energy, i.e., it is stable against these two orthorhombic distortions individually. These results suggest that the β-Sn structure might be metastable, which would explain why the β-Sn structure has been reported in may previous experiments.[3,11,12] Further total-energy calculations were then carried out to estimate the possible energy barrier between the β-Sn and $Imm2$ struc-

tures. However, we found that the β-Sn structure is unstable against the orthorhombic distortion, which increases the a/b ratio and u parameter *simultaneously*. In Fig. 3, we show the calculated total energies as a function of u for various a/b ratios. We note that as the a/b ratio is increased from 1.0, the minimum total energy decreases and the corresponding u deviates from $\frac{1}{4}$. Figure 3 shows that there is a path between the β-Sn and $Imm2$ structure along which the minimum total energy decreases monotonically. However, the minimum total energy decreases rather slowly before the a/b ratio reaches 1.06. For example, the minimum energy for $a/b=1.02$ (u about 0.3) is only 0.2 mRy lower than that of the β-Sn structure. This perhaps explains why the $Imm2$ structure was not found in Ref. 13 even though the stability of the β-Sn structure against orthorhombic distortions appeared to have been investigated.[13] It is well known that the structure of a solid is determined by the free energy $F=E-TS$, where E is the total energy, T the temperature, and S the entropy. Therefore, we speculate that at some high temperatures the β-Sn structure could be stabilized by either the temperature (if the β-Sn structure has a lower entropy than the $Imm2$) or the site disorder, which increases the entropy. So could be a range of the body-centered orthorhombic structures along the minimum energy path shown in Fig. 3. It would be interesting to calculate the entropy of InSb, which is, however, beyond the scope of this paper.

The theoretical zincblende-$Imm2$ transformation pressure can be obtained from Fig. 1 by drawing a straight line that is tangent to both the zincblende and $Imm2$ total-energy parabolas. The slope of this line (the absolute value) is the transition pressure. The theoretical zincblende-$Imm2$ transition pressure thus obtained, is 10.7 kbar. The corresponding transition energy and relative volume change is, respectively, 0.10 eV/unit cell and 23.5%. The zincblende–β-Sn transition pressure would be 13.8 kbar, and the corresponding transition energy is

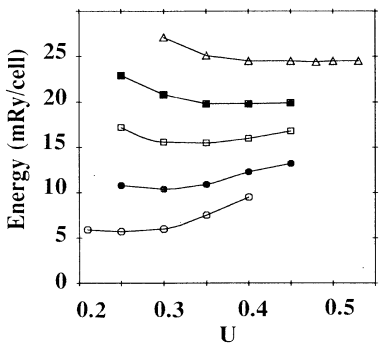

FIG. 3. Calculated InSb total energies (relative to $E=-24\,712.73$ Ry) as a function of u (the position parameter of Sb, see Fig. 2) for various a/b ratios. Open circles, solid circles, open squares, solid squares, and triangles denote calculated total energies, respectively, for $a/b=1.0$, 1.02, 1.04, 1.06, and 1.08. The c parameter (0.561) and the volume (336.1 au^3/cell) are fixed. The total energies for $a/b=1.02$, 1.04, 1.06, and 1.08 are shifted upwards by 5, 10, 15, and 20 mRy, respectively. The curves are the guide to the eye only.

0.13 eV/unit cell and the relative volume change is 23.0%. Experimentally, the transition pressure from the zincblende to the high-pressure structure at room temperature was found to be 22.5 kbar (Ref. 23) and the relative volume change is 19%.[7] Our theoretical zincblende-$Imm2$ transition pressure is much lower (or about 52% too small). The difference in the transition pressure at room and zero temperature is not expected to account for such a larger discrepancy. According to Fig. 1, to increase the theoretical transition pressure to 22.5 kbar, an upwards shift of the $Imm2$ energy-volume curve of as large as 5.0 mRy and a rightwards shift of about 20 a.u.[3] would be needed. (The rightwards shift is to bring the theoretical relative volume change in accord with experiments). A naive conclusion would then be that the LDA severely underestimates the InSb structural energy differences between the zincblende and the high-pressure structure. However, given that the calculated zincblende lattice constant and bulk modulus are in good agreement with experiments, we believe that the LDA is responsible for only part of this large discrepancy. We note that the measured zincblende–β-Sn transition pressure depends sensitively on the type of the applied pressure[12] and also on the rate of pressurization. For example, the transition pressure is about 32 kbar when pure hydrostatic pressure is used, whereas one may obtain a transition pressure as low as 18 kbar under uniaxial pressure.[12] Since the β-Sn structure can be obtained from the zincblende by a simple compression along one of the three (100) axes, uniaxial pressure is perhaps preferred. Because the minimum energy difference between the $Imm2$ and the β-Sn structure is small and also a more complicated nonhydrostatic pressure would be needed to precipitate a low-pressure zincblende-$Imm2$ transition, we would argue that under hydrostatic or uniaxial pressure and at room temperature or above, InSb perhaps first transform to the β-Sn or similar phase before subsequently transforming to the $Imm2$ structure. We note that in an experimental study of the influence of plastic shear deformation on the pressure-induced phase transformation in InSb, a low transition pressure (about 14 kbar) was found.[24] This low-pressure transition could be the direct transition from the zincblende to the $Imm2$. Unfortunately, structural work was not carried out for this phase. It would be interesting and useful to determine the structure of this plastic shear induced phase.

Finally, we note that the calculated transition pressure (33 kbar) from the previous pseudopotential calculations[13] is much larger than the present result (about 14 kbar). This is somehow surprising, since, as mentioned above, the calculated lattice constant and bulk modulus in both cases are in good agreement. As already pointed out in Sec. II, in this work the shallow core states-In (Sb) 4d's were treated as band electrons and were thus fully relaxed. In contrast, in Ref. 13, these states were frozen and their influences were represented by some fixed pseudopotentials (i.e., structurally independent). Because these states have significant charge densities outside the muffin-tin spheres (see Sec. II and also Sec. IV), they are significantly affected by volume changes caused, e.g., by structural phase transformations, and thus their contri-

butions to the structural properties of InSb can not be neglected. This outstanding discrepancy in the transition pressure between Ref. 13 and this work might highlight the importance of taking into consideration the effects of the shallow In (Sb) 4*d* states.

IV. ELECTRONIC STRUCTURES

The InSb band structures for the zincblende, β-Sn, and *Imm*2 structures are shown in Figs. 4(a), 4(b), and 4(c), respectively. These band structures were obtained from the self-consistent potentials using the structural parameters close to the theoretical values. Only the valence and conduction bands are plotted in Fig. 4. The InSb zincblende band structure has been reported before[25,26] but

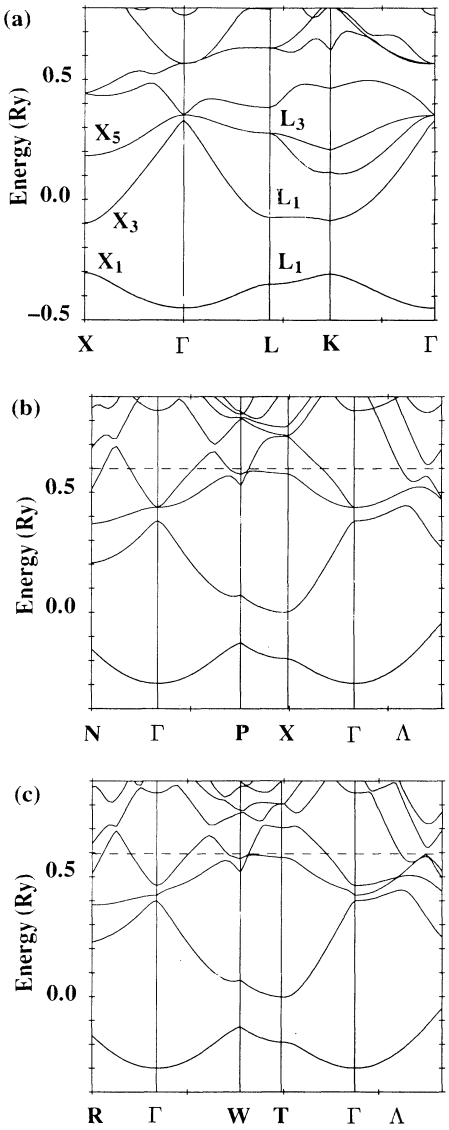

FIG. 4. Calculated InSb band structures for the zincblende (a), β-Sn (b), and *Imm*2 (c) structures. The Fermi energies are 0.353, 0.599, and 0.596 Ry, respectively.

the full potential one has not. Nonetheless, as in Ref. 25, we also find that it turns out to be a semimetal with an exactly vanishing energy gap at the Γ point (the center of the Brillouin zone) [see Fig. 4(a)]. Including the spin-orbit coupling would not make InSb a semiconductor,[26] as our subsequent fully relativistic band-structure calculation using the spherical component of the FLAPW potential and the Korringa-Kohn-Rostoker program,[27] has also shown. Experimentally, InSb is found to have a narrow direct gap of 0.23 eV.[28] It is well known that the density-functional theory is a ground-state theory, and thus, not surprisingly, for many solids especially semiconductors and insulators, there are some significant differences between the LDA conduction bands and the electronic excitation energies.[29] In some cases such as Ge and also InSb considered here, the LDA band structures are semimetallic or metallic, while experimentally these materials are semiconductors. In Ref. 26, the semiconducting gap was corrected empirically. In the present work, our main interest is in the ground-state properties, and we will not deal further with methods to correct the LDA band structures.[29] However, we do find that the valence-band structure of InSb is in good agreement with experiments.[30] For example, the calculated valence-band width is 10.9 eV compared with experimental valued of 11.2 eV [ultraviolet photoemission spectroscopy (UPS)] and 11.7 eV (x-ray photoemission spectroscopy).[30] The valence-band energies (relative to the top of the valence band) for L_3, X_3, and X_1 [see Fig. 4(a)] are 1.0, 6.2, and 8.9 eV, respectively, in good agreement with experimental values of, e.g., 1.1, 6.5, and 9.0 eV (UPS).

The band structures of InSb in the β-Sn and *Imm*2 structures are shown for the first time in Figs. 4(b) and 4(c). Both are metallic, in accord with experiments.[7] Generally speaking, they look rather similar. Some small differences occur because the *Imm*2 structure has a lower symmetry (than the β-Sn structure), which lifts many degeneracies existing in the β-Sn structure. It is not immediately obvious that the *Imm*2 structure is energetically more favorable than the β-Sn structure from view point of the band structure. Figure 4 shows that the structural phase transformation from the zincblende to the high-pressure structures has pronounced effects on the band structure of InSb. Apart from metallization, various band widths and band gaps change significantly. For instance, the valence band width for the β-Sn and *Imm*2 structures are now about 12.2 eV compared with 10.9 eV for the zincblende. The band gap between the first and second valence bands (see Fig. 4) reduces from 2.7 eV to about 0.7 eV. These profound pressure-induced changes in the band structure of InSb may be probed by measurements of electronic properties, such as electronic transport, optical, and photoemission spectroscopies.

Calculated InSb valence charge densities and the differences from the free atomic valence charge densities, are shown as contour plots in Figs. 5, 6, and 7, respectively for the zincblende, β-Sn, and *Imm*2 structures. The covalent bonding is evident in all three cases. Figures 5(b), 6(b), and 7(b) clearly show a considerable charge buildup in the vicinity of the In-Sb bond centers. It is also clear, however, that the covalent bonding is stronger

in the zincblende than in either the β-Sn or the $Imm2$ structure. Like the band structures, the bonding in the the β-Sn and $Imm2$ structures appear to be similar. Table I lists the total, valence, and semicore ($4d$) charges inside the In and Sb muffin-tin spheres. The charges inside the muffin-tin spheres in the the β-Sn and $Imm2$ structures are almost the same but differ from those in the zincblende.

Traditionally, relative stabilities of crystal structures are discussed in terms of the band (or bond) energy (the eigenvalue sum of the occupied states) and the Madelung energy (the electrostatic energy of a system of positive and negative point-charge arrays). As mentioned above, both the calculated band structures and charge-density distributions (covalent bondings) are very similar. Thus, they do not give any obvious clues as why the $Imm2$ structure is more stable than the β-Sn structure. To pursue this stability question further, we looked at the Madelung energies. We found that the $Imm2$ structure has a lower Madelung energy than the β-Sn structure. The calculated Madelung constants (M_{22},M_{12}) (as defined in Ref. 31) are $(-4.5849,-0.8019)$, $(-4.2800,-1.2346)$, and $(-4.4518,-1.2733)$, respectively, for the zincblende, β-Sn, and $Imm2$ structures.

TABLE I. Calculated InSb total, valence, and semicore ($4d$) charges inside the In and Sb muffin-tin spheres. Also included are the corresponding Madelung energies (E_{Mad}) (in the unit of Ry/unit cell) (see text).

		Total	Valence	Semicore ($4d$)	E_{Mad}
zincblende	In	46.951	1.338	9.624	−7.80
	Sb	48.872	2.766	9.962	
β-Sn	In	46.931	1.311	9.628	−12.20
	Sb	48.654	2.712	9.944	
$Imm2$	In	46.929	1.309	9.627	−12.39
	Sb	48.651	2.712	9.942	

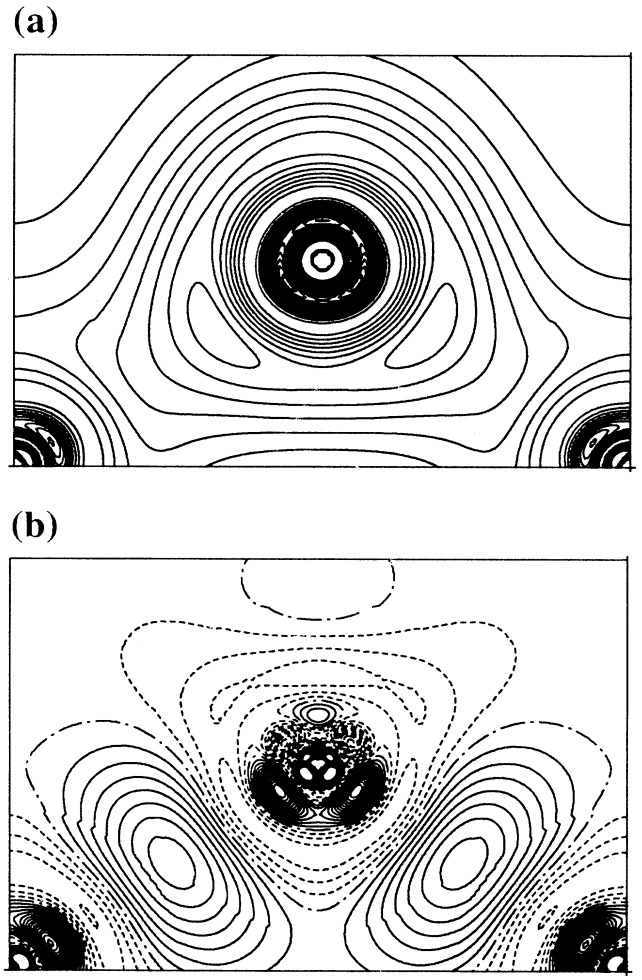

FIG. 5. (110) valence charge densities for InSb in the zincblende structure (a); the differences between the valence charge densities and those obtained by a superposition of the free atomic charge densities (b). The atom near the center is Sb and the atoms on the edges are In. The contour step is 0.05 e/A^3 for (a) and 0.01 e/A^3 for (b). In (b), the dashed curves denote negative contour levels and the dashed-dot contour is set at 0.

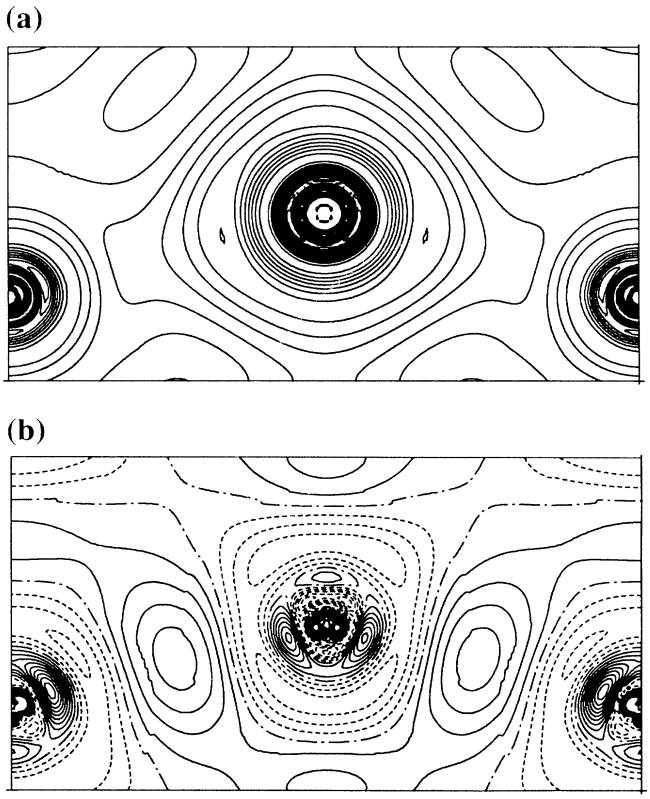

FIG. 6. (010) valence charge densities for InSb in the β-Sn structure (a); the differences between the valence charge densities and those obtained by a superposition of the free atomic charge densities (b). The atom near the center is Sb and the atoms on the edges are In. The contour step is 0.05 e/A^3 for (a) and 0.01 e/A^3 for (b). In (b), the dashed curves denote negative contour levels and the dashed-dot contour is set at 0.

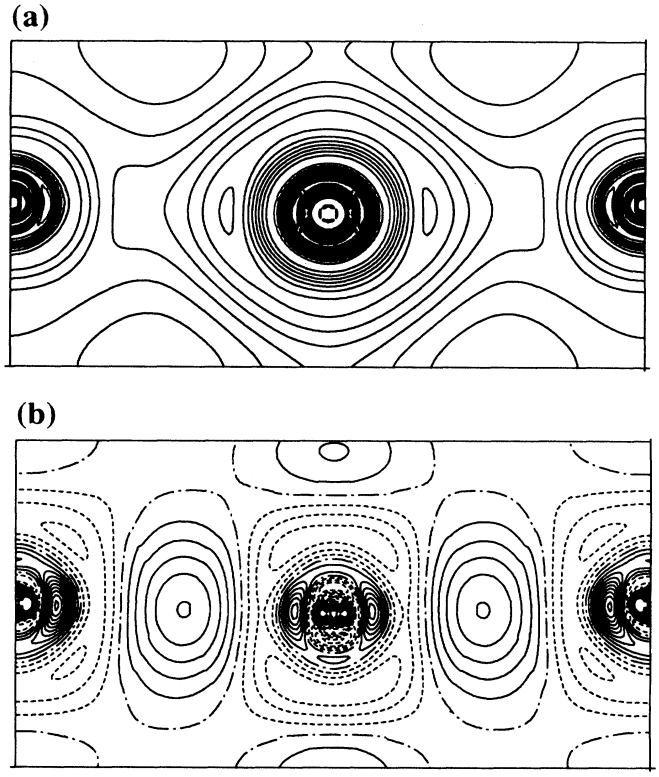

FIG. 7. (100) valence charge densities for InSb in the *Imm*2 structure (a); the differences between the valence charge densities and those obtained by a superposition of the free atomic charge densities (b). The atom near the center is Sb and the atoms on the edges are In. The contour step is 0.05 e/A^3 for (a) and 0.01 e/A^3 for (b). In (b), the dashed curves denote negative contour levels and the dashed-dot contour is set at 0.

They are in the units of the leading lattice constant (a). If the charges inside the muffin-tin spheres in all the cases are assumed to be the same as those in the zincblende structure (Table I), we obtain Madelung energies (E_{Mad}) (defined as the electrostatic energy of a system of ions embedded in a neutralizing uniform background charge density[31]) of −7.80, −11.71, and −11.88 Ry/unit cell for the zincblende, β-tin and *Imm*2 structures, respectively. If the actual calculated charges inside the muffin-tin spheres are used (Table I), Madelung energies obtained are −7.80, −12.20, and −12.39 Ry/unit cell. These simple calculations suggest that the *Imm*2 structure is energetically more favorable than the β-Sn structure mainly because it has a lower Madelung energy. Interestingly, the zincblende structure has a much higher Madelung energy. It is generally believed that the high Madelung energy of the zincblende structure is overcompensated by the low band energy due to the large tetrahedral covalent bonding gap that occurs throughout the Brillouin zone. As the zincblende structure is compressed, the covalency becomes less strong, and eventually the zincblende structure becomes unstable.

In the modern density-functional theory,[14] the total energy of a solid is the sum of three terms, i.e., the kinetic energy (E_{kin}), the Coulombic energy (E_c) and the exchange-correlation energy (E_{xc}). Table II lists the calculated total energies and their decompositions. Indeed, the Coulombic energy is lower in the *Imm*2 structure than in the β-Sn structure. The difference in the Coulombic energy is largely compensated by the higher kinetic energy in the *Imm*2 structure. It is perhaps surprising to see that the zincblende has the lowest Coulombic energy, since it has a highest Madelung energy (see the previous paragraph). In the highly directionally bonded zincblende structure, the electron density tends to be confined in the vicinity of the bond centers where the electrostatic potential is lowest, to minimize the Coulombic energy. The penalty for this confinement, according to the uncertainty principle of quantum mechanics, is a higher kinetic energy, as our results show (Table II). In the zincblende, the Madelung energy based on the simple point-charge model[31] does not reflect the Coulombic energy of the system.

To make connections with the tradition simple analysis, one may further decompose the kinetic term as the valence eigenvalue sum (E_{band}) and the so-called double counting terms, and also single out the general potential Madelung energy[32] (E_{gMad}) from the Coulombic term. In Table II, we also included the valence-band energies (E_{band}) and the general-potential Madelung energies (E_{gMad}). Again, the (general-potential) Madelung energy is lower in the *Imm*2 structure than in the β-Sn structure, and is the highest in the the zincblende structure (see Table II). As expected, the zincblende has the lowest band energy and the β-Sn structure has a slightly higher band energy than the *Imm*2 structure. Nevertheless, the band energies in Table II should not be taken literally, since they were obtained from the different self-consistent potentials, which are difficult to line up with respect to a common level (say the zero potential). Finally, it should be pointed out that the quantities listed in Table II are not those evaluated at the theoretical minimum energy structures. The minimum total energies are −24 712.7339, −24 712.7243, and −24 712.7263

TABLE II. Calculated InSb total energy and its decompositions [the kinetic term (E_{kin}), the Coulombic term (E_c), and the exchange-correlation energy (E_{xc}) term] (see text) for the zincblende, β-Sn, and *Imm*2 structures. Also listed are the valence-band energies (E_{band}) and the generalized Madelung energies (E_{gMad}). All quantities are in units of Ry/unit cell.

	E_{tot}	E_{kin}	E_c	E_{xc}	E_{band}	E_{gMad}
zincblende	−24 712.733	26 017.009	−50 089.596	−640.171	0.243	−49.070
β-Sn	−24 712.724	26 016.847	−50 089.410	−640.161	1.883	−55.933
*Imm*2	−24 712.726	26 016.916	−50 089.471	−640.171	1.868	−55.965

Ry/unit cell for the zincblende, the β-Sn, and the $Imm2$ structures, respectively.

V. CONCLUSIONS

In order to investigate the high-pressure structural and electronic properties of InSb, we have performed first-principles local density-functional electronic structure and total-energy calculations for the cubic zincblende, tetragonal β-Sn, and orthorhombic $Imm2$ structure using the all-electron full potential LAPW method.[9] The results show that under ambient conditions, InSb will exist in the zincblende structure. The calculated lattice constant (a) and bulk modulus (B_0) are in good agreement with experiments. The most important finding of this work is that in the high-pressure region, the β-Sn structure is unstable with respect to a body-centered orthorhombic ($Imm2$) structure. The calculated zincblende-$Imm2$ transition pressure is 10.7 kbar, being much lower than the measured value of 22.5 kbar.[23] The calculated transition pressure from the zincblende to the β-Sn structure is 13.8 kbar. We, however, argued that when pure hydrostatic or uniaxial pressures are applied, InSb first transforms from the zincblende structure to the β-Sn or similar structure before settling down to the $Imm2$ structure at some higher pressures. A complicated nonhydrostatic pressure would be needed to precipitate a low-pressure zincblende-$Imm2$ transition and we suggest that structural determinations be carried out for the shear deformation induced high-pressure phase found at about 14 kbar.[24]

We have also presented the calculated InSb electronic properties. Both the high-pressure structures considered are metallic and they have similar band structures and covalent bonding. The covalent bonding is evident in the calculated valence charge-density distributions for all three structures studied, but is strongest in the zincblende structure. A simple analysis of the Madelung energies based on the calculated charges inside the In and Sb muffin-tin spheres, suggests that the $Imm2$ structure is energetically more favorable than the β-Sn structure because it has a lower Madelung energy.

While the calculated InSb lattice and bulk modulus for the zincblende structure are in agreement with the previous pseudopotential calculations,[13] the calculated zincblende–β-Sn transition pressure is nearly 60% smaller than the value obtained in Ref. 13. This large discrepancy in the calculated transition pressure, we argued, is due to the relaxing of the In and Sb shallow core states ($4d$'s) in this work.

ACKNOWLEDGMENTS

The authors wish to acknowledge the invaluable assistance of R. J. Nelmes, P. D. Hatton, M. I. McMahon, and R. O. Piltz whose experimental image plate results[8] provided the motivation for this work.

[1] J. Donohue, *The Structure of the Elements* (Wiley, New York, 1974).
[2] A. Jayaraman, R. C. Newton, and G. C. Kennedy, Nature (London) **191**, 1290 (1961).
[3] J. D. Jamieson, Science **139**, 845 (1963); R. E. Hanneman, M. D. Banus, and G. C. Kennedy, Phys. Rev. **130**, 540 (1963).
[4] D. R. Yoder-Short, R. Colella, and B. A. Weinstein, Phys. Rev. Lett. **49**, 1438 (1982).
[5] M. Baublitz, Jr. and A. L. Ruoff, J. Appl. Phys. **53**, 6179 (1982).
[6] S. T. Weir, Y. K. Vohar, C. A. Vanderborgh, and A. L. Ruoff, Phys. Rev. B **39**, 1280 (1989).
[7] S. C. Yu, I. L. Spain, and E.-F. Skelton, Solid State Commun. **25**, 49 (1978).
[8] R. J. Nelmes, M. I. McMahon, P. D. Hatton, J. Crain, and R. O. Piltz, Phys. Rev. B **47**, 35 (1993).
[9] P. Blaha, K. Scwarz, P. Sorantin, and S. B. Trickey, Comput. Phys. Commun. **59**, 399 (1990).
[10] M. T. Yin and M. L. Cohen, Phys. Rev. Lett. **50**, 1172 (1983).
[11] S.-C. Yu and I. L. Spain, J. Appl. Phys. **49**, 4741 (1978).
[12] B. Okai and J. Yoshimoto, J. Phys. Soc. Jpn. **45**, 1880 (1980).
[13] S. B. Zhang and M. Cohen, Phys. Rev. B **35**, 7604 (1987).
[14] P. Hohenberg and W. Kohn, Phys. Rev. **136**, B864 (1964); W. Kohn and L. J. Sham, *ibid.* **140**, A1133 (1965).
[15] S. H. Vosko, L. Wilk, and M. Nusair, Can. J. Phys. **58**, 1200 (1980).
[16] S. Massida, B. I. Min, and A. J. Freeman, Phys. Rev. **38**, 1991 (1988).
[17] M. Weinert, E. Wimmer, and A. J. Freeman, Phys. Rev. B **26**, 4571 (1982); P. Blaha, K. Schwarz, and P. H. Dederichs, *ibid.* **38**, 968 (1988); R. E. Cohen, W. E. Pickett, and H. Krakauer, Phys. Rev. Lett. **62**, 831 (1989).
[18] D. D. Koelling and B. N. Harmon, J. Phys. C **10**, 3107 (1977).
[19] H. J. Monkhorst and J. D. Pack, Phys. Rev. B **13**, 5188 (1976).
[20] F. D. Murnaghan, Proc. Nat. Acad. Sci. U.S.A., **30**, 244 (1944).
[21] R. W. G. Wyckoff, *Crystal Structures* (Interscience, New York, 1963), Vol. 1.
[22] L. J. Slutsky and C. W. Garland, Phys. Rev. **113**, 167 (1959).
[23] M. D. Banus and M. C. Lavine, J. Appl. Phys. **40**, 409 (1969).
[24] M. M. Aleksandrova, V. D. Blank, A. E. Golobokov, and Y. S. Konyaev, Fiz. Tverd. Tela (Leningrad) **30**, 577 (1988) [Sov. Phys. Solid State **30**, 330 (1988)].
[25] A. Svane and E. Antoncik, J. Phys. C **20**, 2683 (1987).
[26] M. Cardona, N. E. Christensen, and G. Fasol, Phys. Rev. B **38**, 1806 (1988).
[27] G. Y. Guo and W. M. Temmerman, in *Applications of Multiple Scattering Theory to Materials Science,* edited by W. H. Bulter, P. H. Dederichs, A. Gonis, and R. L. Weaver (Materials Research Society, Pittsburgh, 1992).
[28] N. W. Ashcroft and N. D. Mermin, *Solid State Physics* (Holt, Rinehart, and Winston, New York, 1976).
[29] R. W. Godby, M. Schluter, and L. J. Sham, Phys. Rev. B **36**, 6497 (1987).
[30] L. Ley, R. A. Pollak, F. R. McFeely, S. P. Kowalczyk, and D. A. Shirley, Phys. Rev. B **9**, 600 (1974).
[31] J. Yamashita and S. Asano, J. Phys. Soc. Jpn. **52**, 3506 (1983).
[32] M. Weinert, E. Wimmer, and A. J. Freeman, Phys. Rev. B **26**, 4571 (1982).